Clinical Biomechanics 107 (2023) 106030

Contents lists available at ScienceDirect

Clinical Biomechanics

journal homepage: www.elsevier.com/locate/clinbiomech

The effect of pathological shoulder rhythm on muscle and joint forces after reverse shoulder arthroplasty, a numerical analysis

Johanna Menze [a,b,*], Louis Leuthard [b], Barbara Wirth [c], Laurent Audigé [c], Enrico De Pieri [b,d], Kate Gerber [a], Stephen J. Ferguson [b,c]

[a] University of Bern, Bern, Switzerland
[b] ETH Zurich, Zurich, Switzerland
[c] Schulthess Klinik, Zurich, Switzerland
[d] Department of Biomedical Engineering, University of Basel, Basel, Switzerland

ARTICLE INFO

Keywords:
Reverse shoulder arthroplasty
Shoulder rhythm
Numerical biomechanics
Patient-specific simulations
Musculoskeletal modelling

ABSTRACT

Background: Compromised abduction ability after reverse shoulder arthroplasty is primarily linked to limited glenohumeral range of motion while scapulothoracic mobility can typically be maintained. Glenohumeral joint forces strongly depend on the resulting scapulohumeral rhythm, however, an association between the acting muscle and joint forces and the subject-specific scapulohumeral rhythm after reverse shoulder arthroplasty has not been established.

Methods: Eleven reverse shoulder arthroplasty patients were divided into groups of poor and excellent abduction ability. Subject-specific models were developed and scaled for each patient using existing motion capture data in AnyBody™. Shoulder muscle and joint forces were obtained using inverse dynamics calculations during shoulder abduction to 100° in the scapula plane. The scapulohumeral rhythm, the resting abduction angle and internal body forces between the outcome groups were compared using a Mann Whitney *U* test.

Findings: The mean glenohumeral and scapulothoracic contribution to overall shoulder abduction for the excellent group was on average 9.7% higher and 21.4% lower, respectively, compared to the mean of the poor group. For shoulder abduction angles between 30° and 60°, the excellent group demonstrated on average 25% higher muscle forces in the anterior deltoid which was significantly higher compared to the poor outcome patients. Scapulothoracic muscle activity did not differ significantly between the two functional groups.

Interpretation: Accordingly, rehabilitation strategies focusing on strengthening the anterior part of the deltoid in particular may improve clinical outcomes.

1. Introduction

Two of the most common shoulder disorders, arthritis and deficient rotator cuff muscles, may lead to pain (Boileau et al., 2005), reduced physical activity and reduced quality of life (Gutierrez et al., 2007). Once conservative treatments are exhausted, reverse shoulder arthroplasty (RSA) is a widely used procedure to relieve chronic pain and provide functional improvement (Bergmann et al., 2008; Samitier et al., 2015; Walker et al., 2015). The non-anatomical, reverse ball-and-socket design provides joint stability (Boileau et al., 2005) and counterbalances the deficient rotator cuff by increasing the lever arm of the deltoid muscle (Friesenbichler et al., 2020). However, various intra- and post-operative complications such as scapular notching (Familiari et al., 2018; Petrillo et al., 2017), instability (Familiari et al., 2018; Marzel et al., 2020) and deltoid muscle dysfunction (Bergmann et al., 2008; Familiari et al., 2018; Lee et al., 2016; Marzel et al., 2020) have been reported, which can result in limited external and internal rotation (Petrillo et al., 2017) and inconsistent shoulder flexion and abduction angles. Revisions lead to lower range of motion compared to primary placed prostheses, mainly due to glenohumeral mobility (Alta et al., 2011). Poor outcome in patients has been associated with a limited glenohumeral abduction ability, while the scapulothoracic mobility could be maintained (Friesenbichler et al., 2020; Matsuki et al., 2021). Consequently, the scapulohumeral rhythm (SHR), defined as the ratio of glenohumeral (GH) over scapulothoracic abduction contribution is altered for patients with RSA (Walker et al., 2015; Zdravkovic et al.,

* Corresponding author at: University of Bern, Medical Faculty, School of Biomedical and Precision Engineering, Güterstrasse 24/26, 3008 Bern, Switzerland.
E-mail address: johanna.menze@unibe.ch (J. Menze).

https://doi.org/10.1016/j.clinbiomech.2023.106030
Received 11 January 2023; Accepted 12 June 2023
Available online 14 June 2023
0268-0033/© 2023 The Authors. Published by Elsevier Ltd. This is an open access article under the CC BY license (http://creativecommons.org/licenses/by/4.0/).

2020). Previous research has revealed that the glenohumeral joint forces are related to the scapulohumeral rhythm (Flores-Hernandez et al., 2019), however, an association between the acting joint forces and the subject-specific scapulohumeral rhythm after RSA has not been established. Furthermore, knowledge about the underlying shoulder muscle functionality after RSA, that could help to explain the differences in patient mobility after RSA with varying shoulder rhythms, is lacking to date.

Electromyography (EMG) allows for measurements of the muscle activation patterns to assess muscle functionality. It is a valuable tool to compare functional groups and has revealed significantly altered activation profiles of shoulder muscles for RSA patients compared to control subjects (Pelletier-Roy et al., 2021; Smith et al., 2020; Walker et al., 2014). Direct comparisons between groups are, however, limited as differences in activation patterns can also result from pain or weakness induced compromised maximum isometric contraction which is required to normalize EMG data. Besides, results based on surface electrodes may be distorted by noise and superposition of signals and are therefore limited to capture activation patterns of subcutaneous muscles. Intramuscular deep wire electrodes decrease this error but impose the additional risk of invasive measurement and possibly alter motion resulting from pain (Young et al., 1989). Alternatively, musculoskeletal models are valuable tools to calculate the muscle forces for a given kinematic input and the resultant joint forces. Driven by external kinematic data, the model computes the subject-specific segmental kinematics (Andersen et al., 2009), which can be further used to derive the required muscle forces through inverse dynamics calculations (De Pieri et al., 2018). While musculoskeletal models calculate the minimally required recruitment of muscle forces to perform given kinematics, EMG provide information on the actual muscle activation profile, also being able to capture possible co-contraction of antagonists that could hinder mobility. Thus, investigation by both approaches is useful in gaining understanding of the biomechanics after reverse arthroplasty.

As it remains challenging to accurately capture scapula kinematics based on skin markers, state-of-the-art musculoskeletal shoulder models commonly rely on a generic shoulder rhythm, coupling the scapula and clavicle orientation to humerus kinematics based on linear regression equations derived for healthy subjects (de Groot and Brand, 2001). However, little information exists on muscle and joint forces in pathological cases where the scapulohumeral rhythm is known to deviate from the one defined for healthy subjects.

So far, inverse dynamic musculoskeletal modelling has not been used to compare muscle function between different outcome groups of RSA patients, considering the subject-specific shoulder rhythms. Thus, motion capture driven models of RSA patients are necessary to study the effect of individually altered shoulder rhythms on muscle and joint forces. Such analyses may help to identify the cause of patient deficiencies in range of motion, which could allow personalized rehabilitation strategies to be developed. Moreover, a better understanding of the joint forces in shoulders with reverse prostheses is important to further improve clinical outcomes.

Herein, we present the effect of varying SHR on muscle and joint forces in poor and excellent outcome RSA patients as calculated with subject-specific musculoskeletal models using existing motion capture data. We hypothesise that RSA patients with poor outcome show a significantly altered muscle activation and resulting glenohumeral joint forces compared to excellent outcome RSA patients.

2. Methods

The presented analysis is based on retrospective data acquired by Friesenbichler et al. (2021) to answer if scapulothoracic mobility is affected after reverse shoulder arthroplasty (Friesenbichler et al., 2020). While the previous study solely focused on analysing kinematic data of RSA patients at maximum abduction angle, the following evaluation will consider the continuous motion capture data to 100° abduction in the scapular plane which is used as a kinematic input for the subsequent calculation of muscle and joint forces.

The further use of the data has been approved by the cantonal ethics committee (BASEC Nr. 2020–02123). The complete information on patient selection and exclusion criteria can be found in the reference study by Friesenbichler et al. (2021) (Friesenbichler et al., 2020).

2.1. Participants

Eleven patients (7 male, 4 female) with a mean age of 73 years (range 67–84) treated with a primary, unilateral reverse prothesis (Univers Revers™, Arthrex Inc., USA) for rotator cuff arthropathy, primary or posttraumatic glenohumeral osteoarthritis or acute fracture, underwent three dimensional (3D) kinematic analysis (Vicon, Oxford, UK) (Friesenbichler et al., 2020). The neck shaft angle was 135° in all patients, and according to joint size a 36 mm or 39 mm glenosphere size was chosen (Table 1). Patients were selected based on the maximum angle reached during active abduction in the scapular plane and were divided into groups of poor ($\leq 110°$) and excellent abduction capability ($>140°$) at 17.5 ± 6.1 (range 8–27) months after the operation (poor mobility group $n = 5$, excellent mobility group $n = 6$). Exclusion criteria included local adverse events, systematic or rheumatoid arthritis, revision arthroplasty, or body mass index (BMI) above 30 (Friesenbichler et al., 2020).

2.2. Motion-capture data

Reflective skin markers were placed on the upper body according to the extended Heidelberg Upper Extremity model, which includes 13 individual markers, five clusters of four markers and two stick-like markers (Table 2, Fig. 1). The extension of the Heidelberg model implies the application of clusters consisting of four markers each on the acromion and humerus to increase sensitivity in tracking scapulothoracic and glenohumeral motion while applying a minimum amount of markers required in a clinical routine (Rettig et al., 2009; Rettig et al., 2013). Initially, a static calibration trial in the standing position was performed. Subsequently, patients were seated and asked to execute three bilateral arm ab−/adduction cycles in the scapular plane at a self-selected speed and until maximum range of motion. The plane for scapula abduction and angular reference was indicated by marks on the floor. Kinematic data was recorded using a 3D motion capture system consisting of ten cameras sampling at 200 Hz (Vicon Motion System Ltd., Oxford, UK). Markers were labelled and corrected using Vicon Nexus software (Version 2.6, Oxford Metrics Inc., Oxford, UK) when automated marker identification failed. The corrected marker tracking data was then exported in C3D files for further kinematic and kinetic analysis in a musculoskeletal modelling software. In addition to the motion capture data, body height and weight and information about the affected shoulder side were recorded.

2.3. Musculoskeletal modelling

Subject-specific shoulder models were developed for each patient using a commercially available musculoskeletal simulation software (AnyBody V. 7.3.1, Technology A/S, Denmark) and the AnyBody™ managed modelling repository (AMMR) V. 2.2.3. The humerus, scapula and clavicle connected by the joints define the shoulder model. The glenohumeral joint allows for three degrees of freedom (DOF) in rotation but no translations. Spherical joints connect the clavicle to the thorax (sternoclavicular joint) and the scapula to the clavicle (acromioclavicular joint), respectively. Two additional sliding points are defined between the scapula and the rib cage and a constant distance between the clavicle and the scapula (conoid ligament). Medialization of the glenohumeral centre of rotation due to the reverse prostheses design were not considered. The shoulder joints are spanned by 16 muscles

Table 1
Patient information.

Patient #	Outcome group	Gender	Age	BMI	Body-weight (kg)	Neck Shaft Inclination (°)	Glenosphere size (mm)	Cup size, Inlay size	Stem size	Spacer	Passive Glenohumeral Abduction RoM of affected shoulder (°)	Time between operation and measurement (months)
01	Excellent	Male	75	25	86	135	39	39 39 + 6	9	none	80	16.3
02	Excellent	Male	72	25	65	135	39	39 39 + 3	9	none	75	18.2
03	Excellent	Male	71	26	83	135	39	39 39 + 3	11	none	90	18.8
04	Excellent	Female	76	22	55	135	36	36 39 + 3	9	none	90	8.4
05	Excellent	Female	71	22	63	135	36	36 39 + 3	9	none	70	23.5
06	Excellent	Male	67	24	73	135	39	39 39 + 3	11	none	95	27.1
07	Poor	Female	77	26	65	135	36	36 + offset 39 + 3	6	none	65	16.8
08	Poor	Female	70	29	72	135	36	36 + offest 39 + 3	7	none	60	25.7
09	Poor	Male	84	23	71	135	36	36 39 + 3	9	none	60	14.2
10	Poor	Male	69	25	83	135	39	39 39 + 3	13	none	70	8.9
11	Poor	Male	68	29	83	135	39	39 39 + 3	8	none	80	15.1

Table 2
Marker name, anatomical placement, segment and marker type applied in the extended Heidelberg Upper Extremity model.

Marker name	Anatomical placement	Segment	Marker type
SACR	Midway between the posterior superior iliac spines	Pelvis	Single marker (1)
RASI /LASI	Anterior superior iliac spine, right/left side	Pelvis	Single marker (1)
STRN	Xiphoid process	Thorax	Single marker (1)
THRX 1–4	3 cm below CLAV	Thorax	Marker cluster (4)
CLAV	Jugular notch	Thorax	Single marker (1)
TH10	Spinous process of T10	Thorax	Single marker (1)
C7	Spinous process of C7	Thorax	Single marker (1)
R/L SCAP1–4	Top of the acromion, right/left side	Scapula	Marker cluster (4)
R/L HUM 1–4	Tuberositas deltoidei, right/left side	Humerus	Marker cluster (4)
R/L ELB	Ulna distally to the olecranon, right/left side	Ulna	Stick-like cluster (2)
R/L RAD	Processus styloideus radii	Radius	Single marker (1)
R/L ULN	Processus styloideus ulnae	Ulna	Single marker (1)

which are discretized into 118 muscle bundles to cover the range of muscle origin and insertion points. Muscle strength was directly proportional to its physiological cross sectional area and assumed to be independent of the apparent muscle length during motion [33].

The modelling system uses an inverse dynamic approach to calculate required muscle forces and resultant joint reaction forces for a given kinematic input. As the shoulder is an overdetermined system, whereby multiple muscles generate a force and the associated moment in one DOF, a third order polynomial cost function determines the optimal muscle recruitment and muscle force distribution (Andersen, 2021).

To achieve subject-specific simulations, the models were scaled according to the respective patient height and weight. Bone size in the upper body, trunk and pelvis were further specified based on the specific marker positions in a static reference trial. The patient's motion capture data defined the kinematics of the scapulothoracic, glenohumeral and elbow joint. The kinematic data was imported from trial specific C3D files and marker trajectories were filtered using a second-order low pass Butterworth filter with a cut-off frequency of 3 Hz. To allow for subject-specific scapula motion, the generic scapulohumeral rhythm was inactivated. Kinematic tracking of the segments was solved with a least-squared-optimization between the measured marker trajectories and the virtual markers that were implemented in the respective location of the connected model segment while not violating the kinematic constraints imposed by the joints. The optimization was performed for the whole duration of the trial while the glenohumeral and scapulothoracic joints removed the respective degrees of freedom outlined in the kinematic joint definition. The resultant glenohumeral abduction joint angles, scapulothoracic rotation angles and overall arm abduction angles were subsequently analysed according to the International Society of Biomechanics (ISB) standard (Wu et al., 2005). Kinematic data, muscle and joint forces were analysed and compared among the patients up to shoulder abduction angles of 100° as skin marker induced errors for tracking of scapular kinematics increase with higher shoulder abduction angles.

2.4. Statistical analysis

Scapulohumeral kinematics and muscle and joint forces were presented against shoulder abduction angles for the poor and excellent outcome group. Muscle and joint forces were normalized by body weight (%BW) to minimize intergroup differences in forces from body weight and compare force differences resulting from kinematics. Mean body weight per group were provided to derive acting joint and muscle loads. Statistical comparison between the poor and excellent groups were performed using statistical parametric mapping (SPM). A Mann Whitney *U* test was used throughout the motion as the assumption of normality and equal standard deviations were violated.

Differences in mean values of resting abduction angles (the initial angle between the humerus and thorax before patients started shoulder

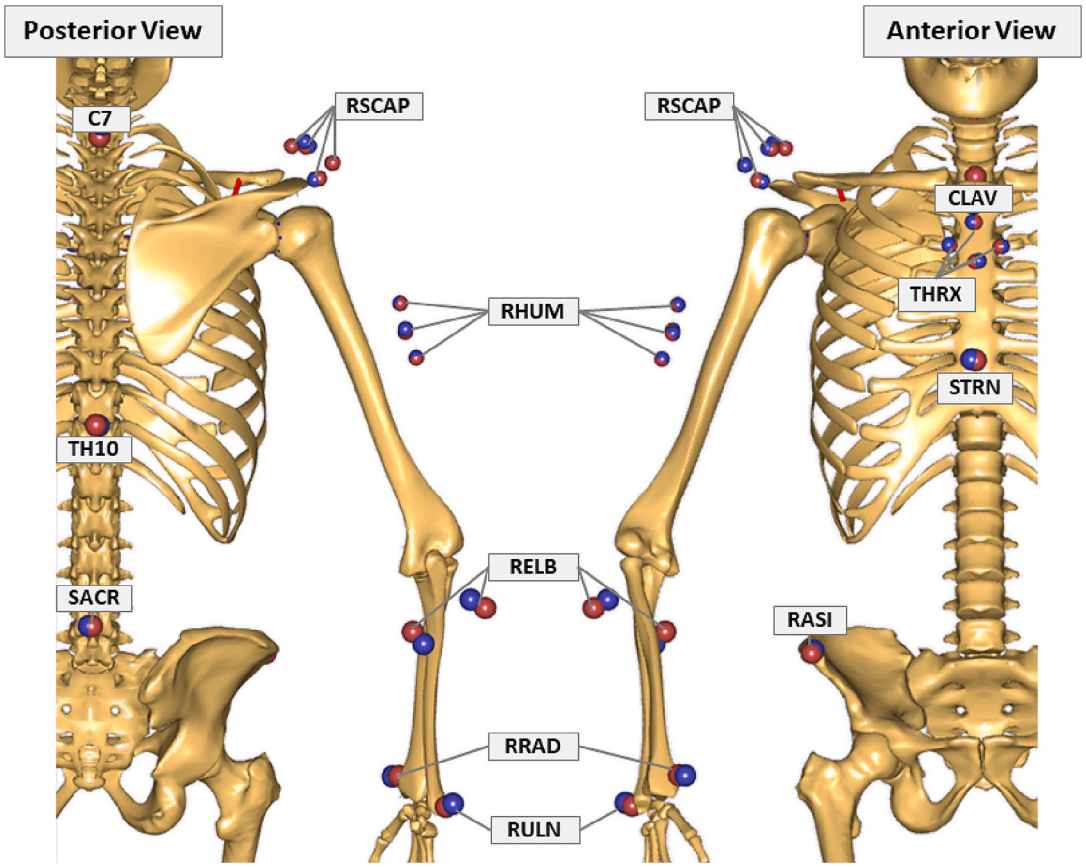

Fig. 1. Anterior and posterior view of the subject-specifically scaled model using the extended Heidelberg Upper Extremity marker protocol.

abduction) between the poor and excellent group, were analysed using a two-tailed Mann Whitney *U* test. The Shapiro-Wilk test was used to verify normality. The level of statistical significance was set to $p < 0.05$.

3. Results

3.1. Kinematics analysis

Glenohumeral abduction (GH) and scapulothoracic (ST) rotation angles are displayed in Fig. 2 (A). GH abduction constantly increased with overall shoulder abduction, whereas ST remained approximately consistent with a slight increase between 70° and 100°. Although no

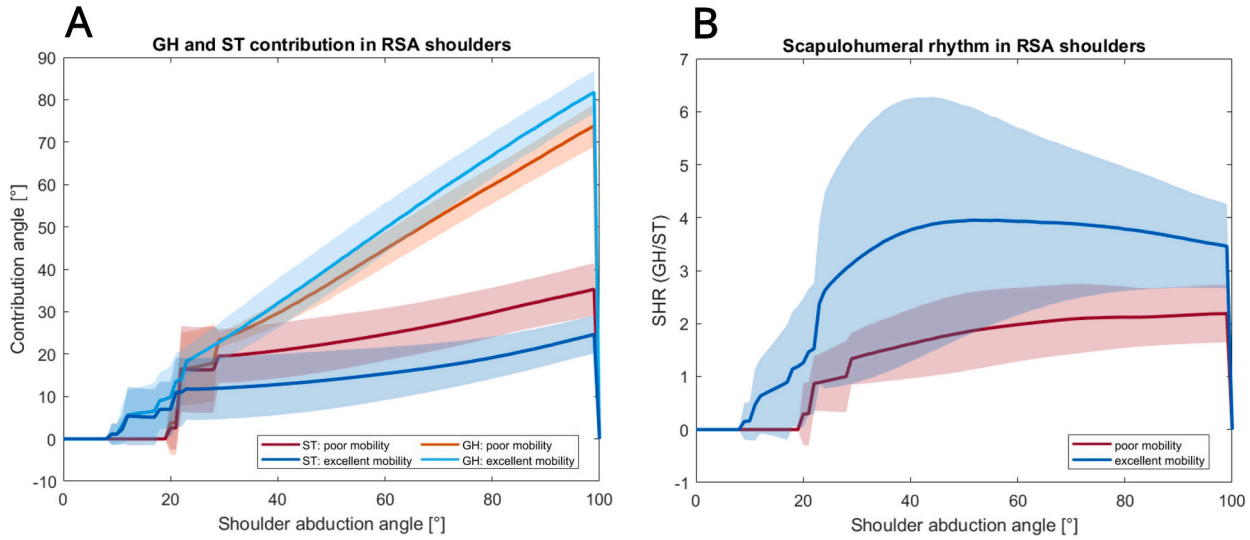

Fig. 2. Comparison of shoulder kinematics between poor and excellent mobility group during shoulder abduction.
A Glenohumeral abduction (GH) and scapulothoracic rotation (ST) in the poor and excellent mobility groupB scapulohumeral rhythm (SHR), the ratio of glenohumeral abduction to scapulothoracic rotation. Curves are represented as mean ± SD. Poor mobility group $n = 5$. Excellent mobility group $n = 6$.

significant difference could be found, the mean for the excellent group showed on average 9.7% (min = 2.4%, max = 12.0%) more GH, and 21.4% (min = 18.0%, max = 25.6%) less ST contribution than the mean of the poor group, once all patients started shoulder abduction (30°).

Subsequently, GH and ST contribution angles were combined in the ratio GH/ST and displayed as SHR in Fig. 2 (B). Large variability in SHR among patients in the excellent group were observed, especially between 30° and 70° shoulder abduction. During shoulder abduction, the mean SHR for the excellent and poor groups remained >3.1 and 1.3, respectively.

Although no significant difference was found, a tendency of higher resting abduction angles (range 11.6° - 30.3°, *p*-value: 0.052) for the poor group is shown in Fig. 3.

3.2. Muscle forces

Fig. 4 (A,B) shows the calculated muscle force in %BW of the main contributors (anterior and lateral deltoid) to GH motion over the course of shoulder abduction as well as the statistical analysis of the anterior deltoid (C, Fig. 4). Mean body weight of the poor and excellent outcome group were 74.8 kg and 70.8 kg, respectively. The analysis did not reveal any significant differences and no clear trend for the comparison of lateral deltoid forces (B) between the two groups. For shoulder abduction angles between 30° and 60°, significant differences in anterior deltoid forces were found between the two groups (A, C). In addition, the excellent group required on average 25.4% (min = 2.7%, max = 61.2%) more muscle forces after commencement of shoulder abduction.

Muscle forces for the inferior and superior trapezius and serratus anterior are shown in Fig. 5 against the course of the subject specific shoulder abduction angle. No significant differences between the excellent and the poor groups were revealed for either of the muscles.

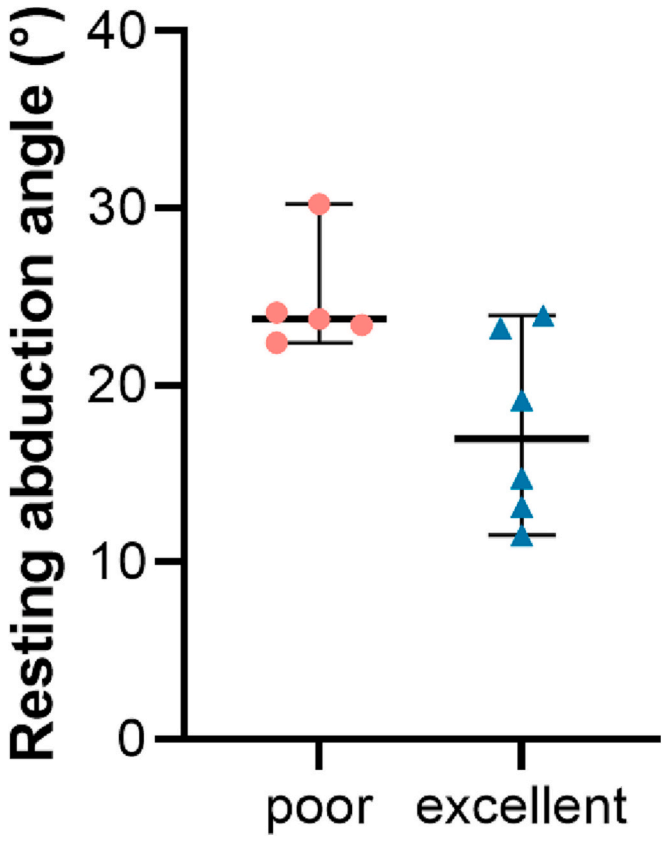

Fig. 3. Resting abduction angles between poor and excellent mobility group. Poor mobility group $n = 5$. Excellent mobility group $n = 6$. Point plots are represented as median ± range.

However, a clear trend with on average 11.9% (min = 0.2%, max = 20.0%) higher required muscle forces of the inferior trapezius (A) in the poor group was observed. The superior trapezius showed low muscle forces (<7% BW) in both groups (B). The serratus anterior (C) was continuously recruited with muscle forces of approximately 10% BW throughout shoulder abduction in both groups.

3.3. Joint reaction forces

Fig. 6 shows glenohumeral joint reaction (GHJR) forces and the statistical analysis of superior shear forces (E). Although a small trend towards higher resultant (A) and compressive (B) forces for the excellent group can be seen, no significant differences were found. For multiple shoulder abduction angles between 20° and 50°, significant higher superior shear forces (C) for the excellent group were revealed. The highest level of superior shear forces appeared at approximately 60° shoulder abduction angle, quickly decreasing afterwards.

4. Discussion

Previous research has shown that SHR varies among clinical outcome groups and limited abduction is associated with compromised GH contribution after RSA (Friesenbichler et al., 2020). However, these findings could not be linked to varying muscle activities assessed by skin-mounted electrodes. Therefore, the current study aimed at identifying differences between mobility groups by computing muscle and joint forces with musculoskeletal models. We thereby focused on subject-specific models considering the SHR.

Knowledge about GH and ST contribution to SHR during motion aids the comprehension of the subject-specific biomechanics with RSA. Previous research has demonstrated on average three times higher GH than ST contribution in healthy controls above 30° abduction (Walker et al., 2015). In comparison, our study revealed a SHR of minimally 3.1:1 above 30° abduction for the excellent mobility group, indicating that a restored SHR correlates with good clinical outcomes after RSA. However, large variability of SHR within the excellent mobility group illustrates the importance of considering subject-specific movement patterns. Especially at lower abduction angles, high SHR might be caused by a medial scapular rotation, resulting in negative ST values. This fits well with the findings of Zdravkovic et al. (2020) who detected medial scapular rotation even before humerus abduction was apparent (Zdravkovic et al., 2020). The decreased GH contribution in the poor group highlights the findings of Friesenbichler et al. (2020), where limited range of abduction correlated with poor GH motion (Friesenbichler et al., 2020). Consequently, it was suggested that patients must compensate with more ST contribution, leading to relatively low SHR values (at minimum 1.3:1 above 30° abduction).

The resting abduction angle is also referred to as an adduction deficit (Gutiérrez et al., 2008). Commonly, this deficit is linked to impingements of the implant on the scapular neck, which has also been shown to correlate with worse clinical outcomes (Simovitch et al., 2007). Our findings agree with Simovitch et al. (2017), showing that the poor group started, on average, at higher angles of shoulder abduction (Simovitch et al., 2007). Neck-shaft angle and glenosphere size were similar among the two groups and as such, they cannot explain the observed differences. A tendency towards higher BMI in the poor mobility group could be an underlying reason for the increased adduction deficit. However, a more detailed analysis would be required to explain the differences based on the implant related factors, such as the inferior glenosphere position and lateral offset of COR (Gutiérrez et al., 2008).

The comparison of apparent muscle forces between the poor and excellent outcome group highlights that there is a relationship between subject-specific SHR and muscle forces. When looking at the muscles contributing to GH motion, especially the anterior deltoid demonstrates its importance for clinical outcomes, as the inverse dynamics analysis revealed significantly higher forces in the excellent outcome group.

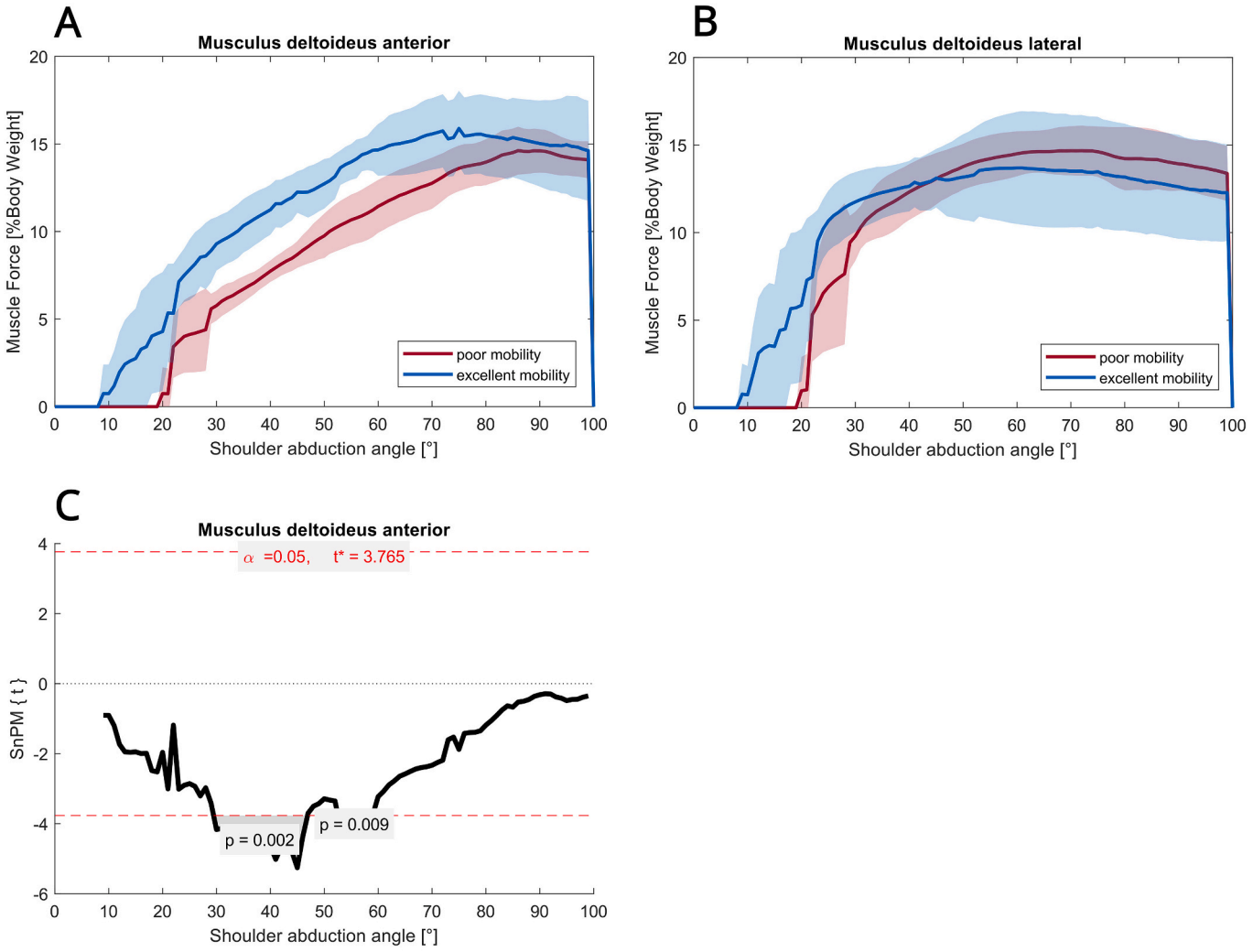

Fig. 4. Comparisons of muscles forces between poor and excellent mobility group during shoulder abduction.
A *M. deltoideus* anterior. B *M. deltoideus* lateral. Curves are represented as mean ± SD. C SnPM = Statistical non-Parametric Mapping of *M. deltoideus* anterior. Curve represents test statistic. Poor mobility group $n = 5$. Excellent mobility group $n = 6$.

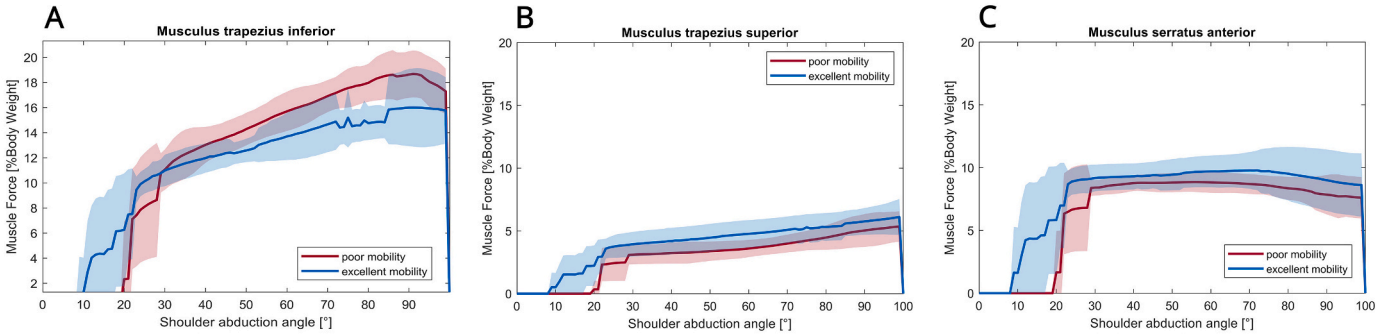

Fig. 5. Comparisons of scapulothoracic muscles forces between poor and excellent mobility group during shoulder abduction.
A *M. trapezius* inferior. B *M. trapezius* superior. C *M. serratus* anterior. Curves are represented as mean ± SD. Poor mobility group $n = 5$. Excellent mobility group $n = 6$.

Pelletier-Roy et al.(2021) reported similar anterior deltoid activity measured in EMG of RSA patients and control subjects. Muscle activity patterns were not associated with distinct shoulder rhythm characteristics but good overall shoulder mobility in the RSA group was reported (Pelletier-Roy et al., 2021). This, consequently agrees well with our finding that anterior deltoid functionality should not be compromised for excellent outcome after RSA. With this, we possibly also found an explanation for the reduced active glenohumeral ROM in revision RSA compared to primary RSA as reported by Alta et al.(2011), as revision could have additionally compromised anterior deltoid functionality (Alta et al., 2011). Walker et al. (2014) observed higher deltoid activity in RSA compared to the control group and argued that the underlying

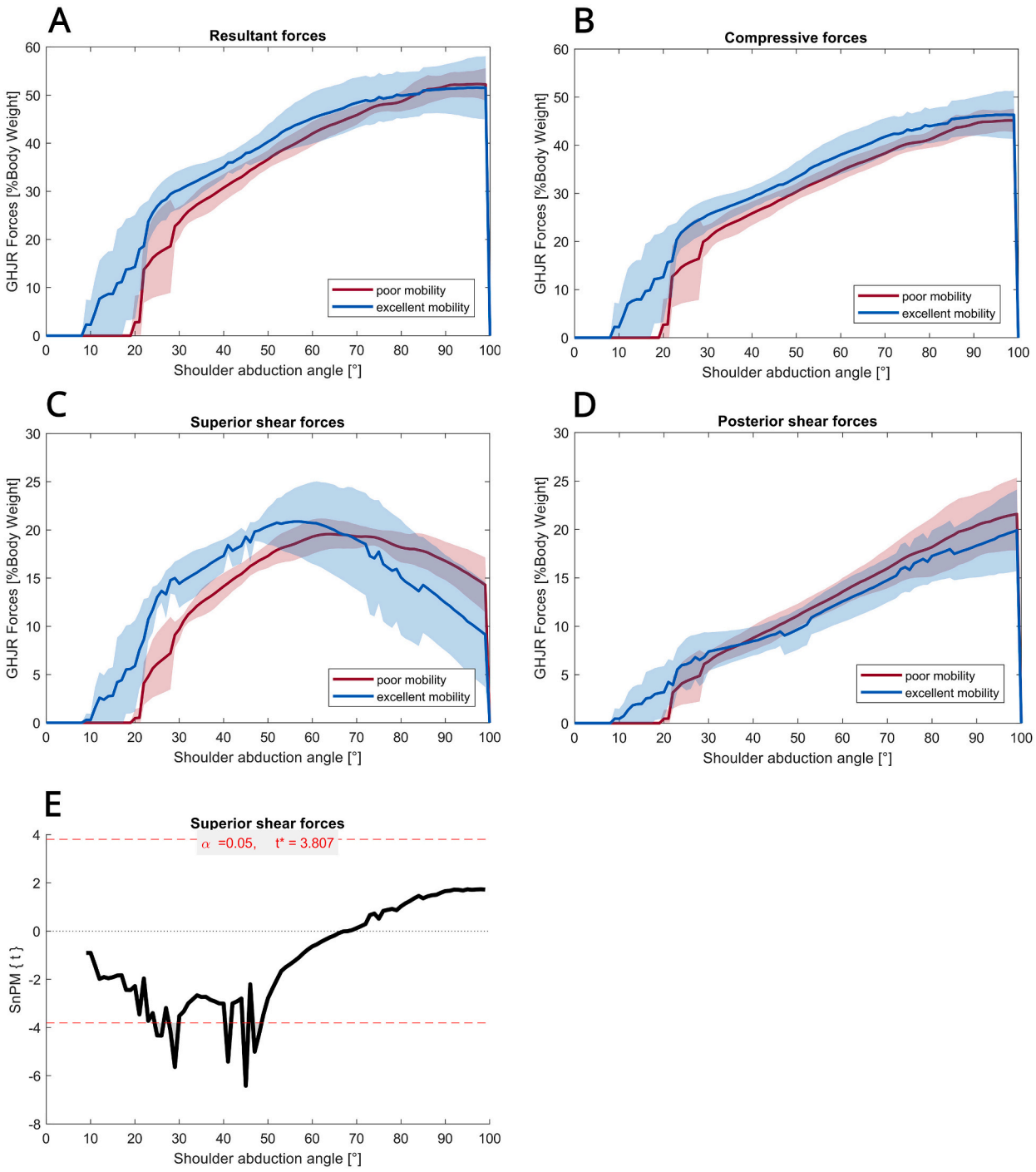

Fig. 6. Comparisons of glenohumeral joint reaction forces between poor and excellent mobility group during shoulder abduction.
A Resultant forces. B Compressive forces. C Superior shear forces. D Posterior shear forces. E SnPM = Statistical non-Parametric Mapping of superior shear forces. Curves are represented as mean ± SD and test statistic, Poor mobility group n = 5. Excellent mobility group n = 6.

reason might be the lost rotator cuff functionality (Walker et al., 2014). Since we did not inactivate the rotator cuff muscularity this hypothesis cannot be confirmed based on our results. The analysis of the ST muscles suggests that patients must compensate with more ST contribution, if the GH motion is limited. In particular, the inferior trapezius showed higher muscle forces for the poor group, indicating its relevance for compensation. Walker et al.(2014) reported consistently stronger trapezius activity pattern for RSA versus control shoulders during all tasks (Walker et al., 2014). The finding that RSA patients present with a stronger ST contribution to shoulder motion (Walker et al., 2015) is consistent with our observation of increased ST muscle forces compensating for compromised GH mobility. However, this cannot be confirmed as muscle activity pattern and ST and GH contribution to overall shoulder kinematics were not measured simultaneously by Walker et al.(2014) (Walker et al., 2014).

Our results of GH joint reaction forces did not enable new conclusions to be drawn due to the large and inconsistent variability. Nonetheless, significantly higher superior shear forces at lower abduction angles for the excellent group were found. These findings are in contradiction to the study of Flores-Hernandez et al. (2019), who

showed that increased ST contribution lead to higher GH joint reaction forces (Flores-Hernandez et al., 2019). However, they further demonstrated that body height, humeral head radius and acromiohumeral interval also influence GH joint reaction forces, which were not investigated in this study.

General limitations of this study are the small sample size, limiting statistical power, as well as the use of only one available shoulder abduction trial per subject. This increases the dependency of the patient-specific modelling result on the selected trial including the effect of trial specific errors. However, there were no systematic differences in patient selection or implant specifications between the excellent and poor outcome group. Furthermore, the periods between operation and kinematic assessment were similar (poor: 16.1 ± 6.1, excellent: 18.7 ± 6.4) and in accordance with the range of follow up periods of similar studies on RSA biomechanics (Alta et al., 2011; Jobin et al., 2012; Pelletier-Roy et al., 2021). Patients with a shorter period until kinematic assessment were, however, likely still recovering from the primary revision, such that rehabilitation was not completed and outcome classification might have not been performed in the final state. In particular, two patients had a follow-up period of <12 months, however, they were distributed into both outcome groups, therefore, the comparison among them should not be biased.

In this study we compared excellent and poor outcome RSA patients. A cohort of healthy age-matched individuals or a cohort of average outcome patients, would provide further meaningful information. In particular, the first comparison could represent a true gold standard, against which the performance of RSA in restoring normal shoulder functionality could be benchmarked. A comparison to a cohort of pathological patients that have not yet undergone RSA could also help to describe and quantify how the surgery improves the demands placed on certain muscles compared to a preoperative state. Both will be considered in future work.

Due to soft tissue artefacts, skin markers are limited to reliably track scapular movements at higher shoulder abduction angles than 100° (Lempereur et al., 2014; van Andel et al., 2009). Moreover, patients in the poor outcome group were not able to elevate their arm beyond 110°. Therefore, kinematic analysis and comparison of muscle and joint forces at higher abduction angles (>100°) between the two outcome groups were not feasible. The focus of this inverse dynamic analysis was therefore on motion until 100° of abduction, a region where the scapula tracking system was reliable and reproducible and where a valid comparison between the two outcome groups was possible.

Regarding the implementation of the RSA geometry in the AnyBodyTM shoulder model, the effect of the implant positioning should be considered and adapted in the musculoskeletal model according to subject-specific information and muscle lever arms and moments should be calculated. It should be noted, however, that only minor changes in joint reaction forces were detected in a similar investigation on cup medialisation of hip prostheses (De Pieri et al., 2021). Furthermore, the implementation of the more elaborate Hill muscle model, additionally calculating passive elastic forces by the muscle and tendon tissue, may give a better understanding about the impact of humeral distalization on deltoid muscle strength when subject-specific implant positioning is being considered.

Further, we propose that future work should also consider adaptation of the maximal isometric muscle forces to the subject-specific forces according to abduction strength measurements. Such an analysis may allow more subject-specific conclusions to be drawn, in particular with regards to the impact of abduction strength on muscle activities.

Increased anterior deltoid forces observed in the excellent mobility group suggest that they may be important for good clinical outcomes. Further studies are needed to determine if patients with poor mobility would benefit from rehabilitation strategies focusing specifically on anterior deltoideus strengthening. Next to a possible deficiency of the anterior deltoid, strengthening of scapulothoracic mobility could further help compensate for lost mobility if glenohumeral range of motion cannot be regained. Further EMG studies are needed to differentiate if the compromised glenohumeral mobility in the poor outcome group is a result of anterior deltoid deficiency or increased antagonistic activity. If the latter were the case, rehabilitation could also focus on decreasing the antagonistic muscle recruitment which might be a result of pain prevention or sensitivity of instability by the patient.

5. Conclusion

This study suggests that a compromised glenohumeral contribution to the shoulder rhythm corresponds with reduced anterior deltoid functionality in poor mobility RSA patients. In conclusion, musculoskeletal models driven by subject-specific SHR allow for evaluation of patient-specific limitations and may help to optimize rehabilitation strategies to further improve clinical outcomes of patients.

IRB/Ethical committee approval

Kantonale Ethikkommission Zürich, BASEC-Nr. 2020-02123.

Declaration of Competing Interest

This research was funded by Innosuisse—Swiss Innovation Agency (grant agreement no.: 35656.1 IP-LS).

References

Alta, T.D., Bergmann, J.H., Veeger, D.J., Janssen, T.W., Burger, B.J., Scholtes, V.A., et al., 2011. Kinematic and clinical evaluation of shoulder function after primary and revision reverse shoulder prostheses. J. Shoulder Elb. Surg. 20 (4), 564–570. https://doi.org/10.1016/j.jse.2010.08.022.

Andersen, M.S., 2021. Introduction to musculoskeletal modelling. In: Jin, Z., Li, J., Chen, Z. (Eds.), Computational Modelling of Biomechanics and Biotribology in the Musculoskeletal System, Second edition. Woodhead Publishing Series in Biomaterials: Woodhead Publishing, pp. 41–80 (ISBN No. 978–0–12-819531–4).

Andersen, M.S., Damsgaard, M., Rasmussen, J., 2009. Kinematic analysis of over-determinate biomechanical systems. Comp. Methods Biomechan. Biomed. Eng. 12 (4), 371–384. https://doi.org/10.1080/10255840802459412.

Bergmann, J.H.M., de Leeuw, M., Janssen, T.W.J., Veeger, D.H.E.J., Willems, W.J., 2008. Contribution of the reverse endoprosthesis to glenohumeral kinematics. Clin. Orthop. Relat. Res. 466 (3), 594–598. https://doi.org/10.1007/s11999-007-0091-5.

Boileau, P., Watkinson, D.J., Hatzidakis, A.M., Balg, F., 2005. Grammont reverse prosthesis: design, rationale, and biomechanics. J. Shoulder Elb. Surg. 14 (1 Suppl S), 147S–161S. https://doi.org/10.1016/j.jse.2004.10.006.

de Groot, J.H., Brand, R., 2001. A three-dimensional regression model of the shoulder rhythm. Clin. Biomech. 16 (9), 735–743. https://doi.org/10.1016/S0268-0033(01)00065-1.

De Pieri, E., Lund, M.E., Gopalakrishnan, A., Rasmussen, K.P., Lunn, D.E., Ferguson, S.J., 2018. Refining muscle geometry and wrapping in the TLEM 2 model for improved hip contact force prediction. PLoS One 13 (9), e0204109. https://doi.org/10.1371/journal.pone.0204109.

De Pieri, E., Atzori, F., Ferguson, S.J., Dendorfer, S., Leunig, M., Aepli, M., 2021. Contact force path in total hip arthroplasty: effect of cup medialisation in a whole-body simulation. HIP International 31 (5), 624–631. https://doi.org/10.1177/1120700020917321.

Familiari, F., Rojas, J., Nedim Doral, M., Huri, G., McFarland, E.G., 2018. Reverse total shoulder arthroplasty. EFORT Open Rev. 3 (2), 58–69. https://doi.org/10.1302/2058-5241.3.170044.

Flores-Hernandez, C., Eskinazi, I., Hoenecke, H.R., D'Lima, D.D., 2019. Scapulothoracic rhythm affects glenohumeral joint force. JSES Open Access 3 (2), 77–82. https://doi.org/10.1016/j.jses.2019.03.004.

Friesenbichler, B., Grassi, A., Grobet, C., Audigé, L., Wirth, B., 2020. Is limited shoulder abduction associated with poor scapulothoracic mobility after reverse shoulder arthroplasty? Arch. Orthop. Trauma Surg. https://doi.org/10.1007/s00402-020-03445-z.

Gutierrez, D., Thompson, L., Kemp, B., Mulroy, S., 2007. The relationship of shoulder pain intensity to quality of life, physical activity, and community participation in persons with paraplegia. J. Spinal Cord Med. 3 https://doi.org/10.1080/10790268.2007.11753933.

Gutiérrez, S., Comiskey, C.A., Luo, Z.-P., Pupello, D.R., Frankle, M.A., 2008. Range of impingement-free abduction and adduction deficit after reverse shoulder arthroplasty. Hierarchy of surgical and implant-design-related factors. J. Bone Joint Surg. Am. 90 (12), 2606–2615. https://doi.org/10.2106/JBJS.H.00012.

Jobin, C.M., Brown, G.D., Bahu, M.J., Gardner, T.R., Bigliani, L.U., Levine, W.N., et al., 2012. Reverse total shoulder arthroplasty for cuff tear arthropathy: the clinical effect of deltoid lengthening and center of rotation medialization. J. Shoulder Elb. Surg. 21 (10), 1269–1277. https://doi.org/10.1016/j.jse.2011.08.049.

Lee, K.W., Kim, Y.I., Kim, H.Y., Yang, D.S., Lee, G.S., Choy, W.S., 2016. Three-dimensional scapular kinematics in patients with reverse total shoulder arthroplasty during arm motion. Clin. Orthop. Surg. 8 (3), 316–324. https://doi.org/10.4055/cios.2016.8.3.316.

Lempereur, M., Brochard, S., Leboeuf, F., Rémy-Néris, O., 2014. Validity and reliability of 3D marker based scapular motion analysis: a systematic review. J. Biomech. 47 (10), 2219–2230. https://doi.org/10.1016/j.jbiomech.2014.04.028.

Marzel, A., Schwyzer, H.-K., Kolling, C., Moro, F., Flury, M., Glanzmann, M.C., et al., 2020. The Schulthess local shoulder arthroplasty registry (SAR): cohort profile. BMJ Open 10 (11), e040591. https://doi.org/10.1136/bmjopen-2020-040591.

Matsuki, K., Hoshika, S., Ueda, Y., Tokai, M., Takahashi, N., Sugaya, H., et al., 2021. Three-Dimensional Kinematics of Reverse Shoulder Arthroplasty: A Comparison between Shoulders with Good or Poor Elevation.

Pelletier-Roy, R., Ratté-Larouche, M., Laurendeau, S., Pelet, S., 2021. Electromyographic and kinematic study of reverse total shoulder arthroplasty: an observational prospective cohort study. J. Shoulder Elb. Surg. 30 (1), 165–171. https://doi.org/10.1016/j.jse.2020.04.053.

Petrillo, S., Longo, U.G., Papalia, R., Denaro, V., 2017. Reverse shoulder arthroplasty for massive irreparable rotator cuff tears and cuff tear arthropathy: a systematic review. Musculoskelet. Surg. 101 (2), 105–112. https://doi.org/10.1007/s12306-017-0474-z.

Rettig, O., Fradet, L., Kasten, P., Raiss, P., Wolf, S.I., 2009. A new kinematic model of the upper extremity based on functional joint parameter determination for shoulder and elbow. Gait Posture 30 (4), 469–476. https://doi.org/10.1016/j.gaitpost.2009.07.111.

Rettig, O., Maier, M.W., Gantz, S., Raiss, P., Zeifang, F., Wolf, S.I., 2013. Does the reverse shoulder prosthesis medialize the center of rotation in the glenohumeral joint? Gait Posture 37 (1), 29–31. https://doi.org/10.1016/j.gaitpost.2012.04.019.

Samitier, G., Alentorn-Geli, E., Torrens, C., Wright, T.W., 2015. Reverse shoulder arthroplasty. Part 1: systematic review of clinical and functional outcomes. Int. J. Shoulder Surg. 9 (1), 24–31. https://doi.org/10.4103/0973-6042.150226.

Simovitch, R.W., Zumstein, M.A., Lohri, E., Helmy, N., Gerber, C., 2007. Predictors of scapular notching in patients managed with the Delta III reverse total shoulder replacement. JBJS 89 (3), 588–600. https://doi.org/10.2106/JBJS.F.00226.

Smith, R.A., Woolley, K., Mazzocca, A., Feinn, R., Cote, M., Gomlinski, G., et al., 2020. Kinematics and EMG activity in reverse total shoulder arthroplasty. J. Orthop. 22, 165–169. https://doi.org/10.1016/j.jor.2020.04.017.

van Andel, C., van Hutten, K., Eversdijk, M., Veeger, D., Harlaar, J., 2009. Recording scapular motion using an acromion marker cluster. Gait Posture 29 (1), 123–128. https://doi.org/10.1016/j.gaitpost.2008.07.012.

Walker, D., Wright, T.W., Banks, S.A., Struk, A.M., 2014. Electromyographic analysis of reverse total shoulder arthroplasties. J. Shoulder Elb. Surg. 23 (2), 166–172. https://doi.org/10.1016/j.jse.2013.05.005.

Walker, D., Matsuki, K., Struk, A.M., Wright, T.W., Banks, S.A., 2015. Scapulohumeral rhythm in shoulders with reverse shoulder arthroplasty. J. Shoulder Elb. Surg. 24 (7), 1129–1134. https://doi.org/10.1016/j.jse.2014.11.043.

Wu, G., van der Helm, F.C.T., Veeger, H.E.J.D., Makhsous, M., van Roy, P., Anglin, C., et al., 2005. ISB recommendation on definitions of joint coordinate systems of various joints for the reporting of human joint motion–Part II: shoulder, elbow, wrist and hand. J. Biomech. 38 (5), 981–992. https://doi.org/10.1016/j.jbiomech.2004.05.042.

Young, C.C., Rose, S.E., Biden, E.N., Wyatt, M.P., Sutherland, D.H., 1989. The effect of surface and internal electrodes on the gait of children with cerebral palsy, spastic diplegic type. J. Orthop. Res. 7 (5), 732–737. https://doi.org/10.1002/jor.1100070515.

Zdravkovic, V., Alexander, N., Wegener, R., Spross, C., Jost, B., 2020. How do scapulothoracic kinematics during shoulder elevation differ between adults with and without rotator cuff Arthropathy? Clin. Orthop. Relat. Res. 478 (11), 2640–2649. https://doi.org/10.1097/CORR.0000000000001406.